


## ORIGINAL RESEARCH

# Electromagnetic time reversal for online partial discharge location in power cables: Influence of interfering reflections from grid components

Antonella Ragusa<sup>1,2</sup> | Peter A. A. F. Wouters<sup>3</sup> | Hugh Sasse<sup>1</sup> | Alistair Duffy<sup>1,2</sup>  | Farhad Rachidi<sup>4</sup> | Marcos Rubinstein<sup>5</sup>

<sup>1</sup>Faculty of Computing, Engineering and Media, De Montfort University, The Gateway, Leicester, UK

<sup>2</sup>The Institute of Marine Engineering, Italian National Research Council, Roma, Italy

<sup>3</sup>Department of Electrical Engineering, Eindhoven University of Technology, Eindhoven, The Netherlands

<sup>4</sup>School of Engineering, The École Polytechnique Fédérale de Lausanne, Lausanne, Switzerland

<sup>5</sup>Institute for Information and Communication Technologies, University of Applied Sciences and Arts Western Switzerland, Yverdon-les-Bains, Switzerland

## Correspondence

Alistair Duffy, The Gateway, Leicester, LE1 9BH, UK.

Email: [apd@dmu.ac.uk](mailto:apd@dmu.ac.uk)

## Abstract

In online single-sided partial discharge (PD) location, the measured PD reflection patterns are affected by the characteristics of all the components of the associated power network. This paper analyses the performance of a PD location method based on electromagnetic time reversal (EMTR) theory, when interfering reflections contribute to the transient signals emitted by the PD event. The topology analysed is formed from a ring main unit (RMU) in a medium voltage grid with mixed cross-linked polyethylene and paper-insulated lead-covered (PILC) cable sections. The PD reflection patterns, observed at the RMU, are disturbed by the reflections coming from the impedance discontinuities of the circuit and by the reflections coming from the cable ends of the PILC cables connected to the RMU. The simulated configuration is chosen such that classical location techniques tend to fail due to overlapping peaks and other signal distortion. This is because the classic techniques are based on identifying individual reflection peaks from which the PD source can be determined via differences in time of arrival. The numerical investigation shows that the accuracy of the EMTR-based location method is robust against these effects, achieving a PD localisation with an error less than the 0.1%. The results also show that the EMTR-based method can localise PDs using a PD monitoring point located somewhere along the network and not necessarily at the line termination.

## 1 | INTRODUCTION

The failure of insulation in power cable of distribution and transmission networks can lead to major social and economic consequences. This is because according to the statistics more than 85% of equipment failures are related to insulation damage [1]. The deterioration of the insulation is often associated with the presence of partial discharge (PD) events that are localised electrical discharges [2] starting in defects of the insulation. After a period of activity, PDs can generate undesirable effects ranging from temporary faults to black outs. Therefore, the online localisation of PD sources in power cables is a suitable method to monitor the grid integrity, avoiding faults and improving the reliability of the electrical grid [3].

Online PD location is mostly performed using reflectometry or travelling wave techniques, such as those proposed in [4–7].

These techniques are based on the fact that a PD produces electromagnetic current and voltage pulses that travel towards the cable ends. In the online single-sided PD location method [4, 5], a measurement system, at one cable end, detects the pulse coming directly from the PD source and the pulse reflected from the other cable end. The delay between their peaks allows estimating the location of the PD source. In the double-end [5] and multiple-end [6] location methods, synchronised measurements of the direct PD signals are performed in double or multiple points of the line, and the PD source is localised by the delay of these measurements.

In medium voltage (MV) grids, PD measurement units are installed inside a ring main unit (RMU) as shown in Figure 1 [8]. Typically, an RMU has one to five MV cables connected to it and an MV/low voltage (LV) distribution transformer. The observation point (OP) inside the RMU monitors one or more

This is an open access article under the terms of the [Creative Commons Attribution-NonCommercial-NoDerivs](https://creativecommons.org/licenses/by-nc-nd/4.0/) License, which permits use and distribution in any medium, provided the original work is properly cited, the use is non-commercial and no modifications or adaptations are made.

© 2024 The Authors. *IET Science, Measurement & Technology* published by John Wiley & Sons Ltd on behalf of The Institution of Engineering and Technology.

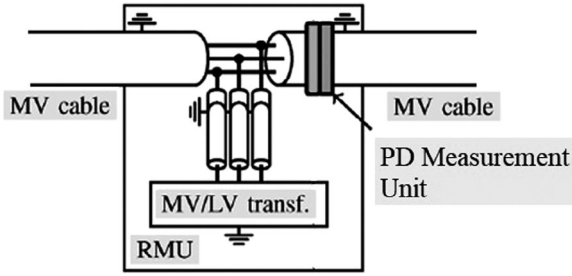


FIGURE 1 RMU with the PD measurement unit [8]. RMU, ring main unit.

cable sections between two RMUs [8]. The effectiveness of the online PD localisation is affected by several issues related to the noise level in an operating grid and the distortion of the PD signals during their propagation along the line. These phenomena make it difficult to properly identify the PD signal peaks, using classical travelling wave-based techniques to localise the PD source [3]. A big challenge in single-sided PD localisation, monitoring a cable in an RMU, comes from the presence of the PD pulses reflected from other cables connected to the same RMU and from the connections at the other far end of the monitored cable. The distribution transformer in the RMU and the cable connecting the transformer to the busbar act as a complex impedance that often allows transmission from the other RMU connected cables. In this situation, the PD return signals affect the measured PD signals at the OP making it difficult to localise the source with traditional methods like signal threshold discrimination.

In previous work [9–11], the authors have shown how PD localisation based on electromagnetic time reversal (EMTR) [10] overcomes the issues related to noise and distortion [10, 11], using only one OP [9]. In [13], the authors have shown that an EMTR-based method is a promising solution to address the issue related to the presence of the PD return signals, proposing a first numerical analysis of its effectiveness in a simple system formed by a cable monitored by an OP to which a second cable is connected. In [13] a simplified analysis was carried out where the presence of an RMU was ignored, and only the interfering effect of the PD reflected signals was considered. In this paper, a more realistic system topology is analysed reproducing the greater complexity of a real operating grid. A mixed cable circuit formed by cross-linked polyethylene (XLPE) and a paper-insulated lead-covered (PILC) three-phase cable section connected to an RMU is used. The XLPE section is also connected, at the other end, to a second PILC cables section. The PD events on the XLPE cables section are monitored by a measurement unit in the RMU. A detailed model of the complex impedance of the cables and of the RMU is used to reproduce the distortion of the PD signals due to the grid components.

The paper is organised as follows. In Section 2, the method based on the EMTR theory is briefly introduced. In Section 3, the adopted models to reproduce the PD signal distortion and the PD reflection pattern due to the grid components, and of the complex impedance of cables and the RMU, are described. Finally, in Section 4 the performance of the EMTR

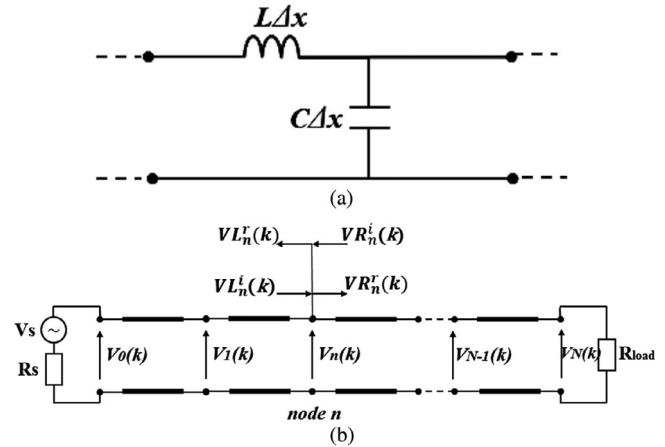


FIGURE 2 Equivalent circuit of a power line node (a) and its 1D TLM model (b) [14]. TLM, transmission line matrix.

method is analysed. The paper ends with conclusions presented in Section 5.

## 2 | TIME REVERSAL METHOD FOR PD LOCALISATION

The EMTR-based method for the PD localisation [9] is based on the invariance under time reversal of the Telegrapher's equations [12], describing the PD signal propagation on power lines, and on the use of the Transmission Line Matrix (TLM) numerical method [14] to solve the Telegrapher's equations in the time reversal domain. A detailed description of the method is reported in [9].

The basic steps of the EMTR-based PD localisation procedure are the following:

1. Measure the PD signal at one OP along the power network.
2. Time-reverse the measured PD signal.
3. Define guessed PD locations (GPDs) in nodes of a 1D TLM model of the network.
4. Simulate the back-injection of the time-reversed PD signal for the different GPDs using the TLM method.
5. Localise the PD source by identifying the GPD characterised by the maximum energy.

The GPD node reproduces the line transverse impedance of the cable modified by the PD event [9]. The TLM numerical method is adopted to describe the time reversal propagation of the PD signals. The EMTR simulations are performed using a lossless 1D TLM model of the system under study. It has been demonstrated that a 1D TLM lossless model is sufficient to provide accurate results for measurements taken from a lossy cable [10]. In the 1D TLM model, the line is discretised into a series of  $N$  segments of length  $\Delta x$  as shown in Figure 2a. Each  $LC$  section is represented by a transmission line with a propagation speed,  $u$ , a characteristic impedance  $Z_c$ , and a transit time,  $\Delta t$ , given by Equations (1) and (2)

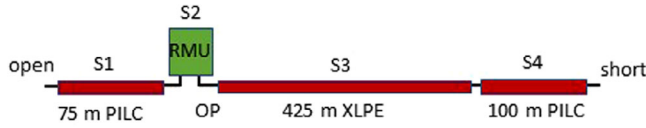


**FIGURE 3** Configuration of the investigated cable configuration including an RMU. RMU, ring main unit.

$$u = \frac{1}{\sqrt{LC}}; \quad Z_c = \sqrt{L/C} \quad (1)$$

$$\Delta t = \frac{\Delta x}{u} = \Delta x \cdot \sqrt{LC} \quad (2)$$

where  $L$  and  $C$  are, respectively, the per-unit-length longitudinal inductance and transverse capacitance of the line.

The 1D TLM equivalent model of the line, obtained connecting the  $N$  sections, is shown in Figure 2b.

For each TR simulation, the energy  $E_n$  stored in the GPD L transverse impedance is evaluated and normalised with respect to the maximum energy

$$E_n = \frac{\frac{1}{2} C_{PD} \sum_{k=1}^M V_{GPD L}^2(k)}{\frac{1}{2} C_{PD} \sum_{k=1}^M V_{GPD L_m}^2(k)} \quad \text{with } M = \frac{T}{\Delta t} \quad (3)$$

where  $V_{GPD L_m}(k)$  is the maximum voltage over all the GPD Ls,  $C_{PD}$  is the GPD L transverse capacitance modified by the PD event [9], and  $M$  the number of the samples. In this work, the first step, which is the experimental measurement of the PD signal in the real network, is substituted by a direct time (DT) simulation of the PD signal propagation in the system under study using a lossy model of the system that is able to reproduce the distortion of the PD signal during the propagation in a real system. It uses real cable design parameters and the modelling of the RMU response is based on measurements at several RMUs [15]. The used lossy model is described in the following section.

### 3 | MODELS OF RMU AND POWER CABLES

The adopted test configuration is the mixed cable circuit shown in Figure 3. The OP is located at the XLPE connection at the RMU. The cable under test is an XLPE cable with length of 425 m connected at its end to a 100-m long PILC cable shorted at the second end. On the other side of the RMU there is a 75-m long PILC cable, opened at the other end. Short cable sections in grids can arise, for example, after repairing a failed connection by replacing the defective part. The inserted cable may have different signal propagation characteristics. The short and open ends represent a worst-case situation guaranteeing high reflection coefficients. The relatively short PILC cables at the ends cause multiple reflections, arriving shortly after each other. They obscure an easy identification of individual peaks. The waveform is further distorted by the presence of an RMU at the OP position. As detection takes place over all three phases, the

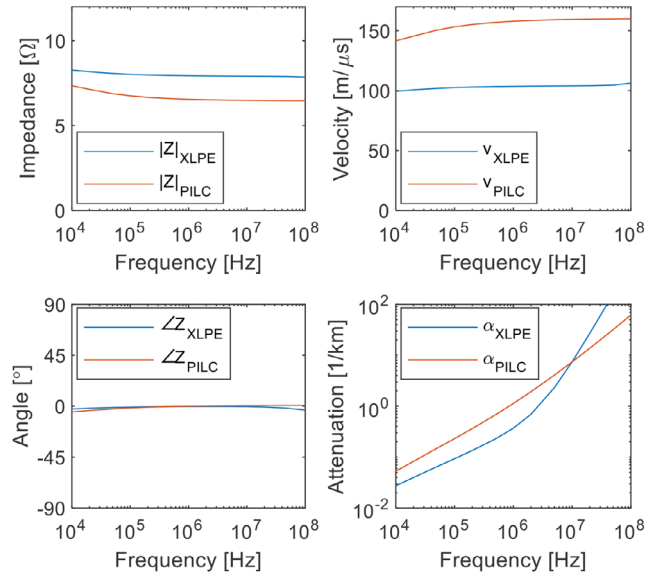


**FIGURE 4** Characteristic impedance, velocity and attenuation for XLPE (blue) and PILC (red) cables. PILC, paper-insulated lead-covered; XLPE, cross-linked polyethylene.

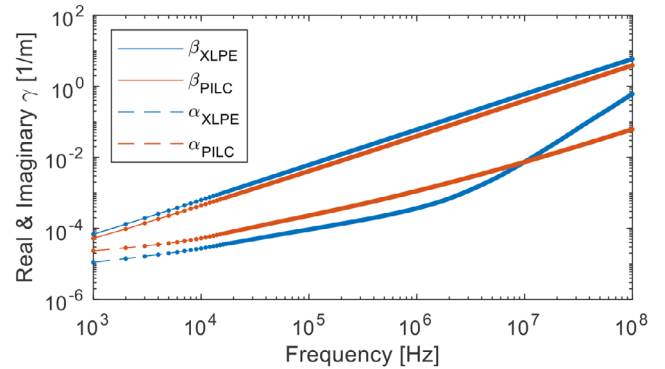


**FIGURE 5** Real and imaginary part of the propagation coefficient for XLPE (blue) and PILC (red) cables; the dots indicate the resampling with frequency steps of 1 kHz. PILC, paper-insulated lead-covered; XLPE, cross-linked polyethylene.

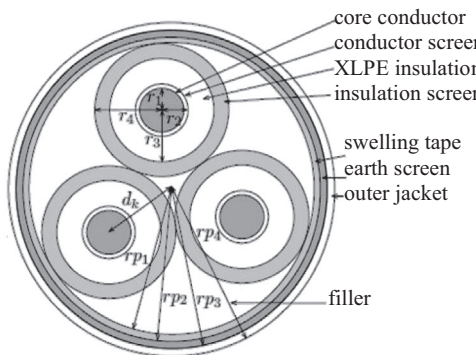
three-phase cables will be modelled as single-conductor cables. Essentially, the topology has been designed to be a challenging test for the proposed method.

In Tables 1 and 2 the characteristics of the XLPE and PILC cables are reported. The modelled cable characteristic impedances, velocities, and attenuation coefficients are shown in Figure 4. In Figure 5, the simulated real and imaginary propagation coefficients (1-2-5 sequence from 1 kHz to 100 MHz) are plotted together with interpolated values (dots), needed for applying the inverse Fourier transforms.

The impedance at the cable ends can be frequency dependent, for example, the input impedance of a consecutive cable or from components in an RMU. The characteristic cable impedance is approximated with a real value, taken as the average of the simulated absolute values between 100 kHz and 10 MHz (these values concern all phases in parallel with respect

TABLE 1 XLPE cable characteristics.

Cable parameters	Value
Al conductors, $r_1$	8.55 mm
conductor screen, $r_2$	9.35 mm
XLPE insulation, $r_3$	12.75 mm
insulation screens, $r_4$	14.00 mm
conductors-centre, $d_k$	16.16 mm
filler material, $r_{p1}$	30.15 mm
swelling tape, $r_{p2}$	30.50 mm
Cu earth screen, $r_{p3}$	31.50 mm
PVC jacket, $r_{p4}$	33.00 mm
conductivity conductor (Al), $\sigma_{Al}$	$3.69 \cdot 10^7$ S/m
conductivity earth screen (Cu), $\sigma_{Cu}$	$5.84 \cdot 10^7$ S/m
relative permittivity XLPE, $\epsilon_{r,xlpe}$	2.26-0.001j
relative permittivity filler, $\epsilon_{r,filler}$	4.0

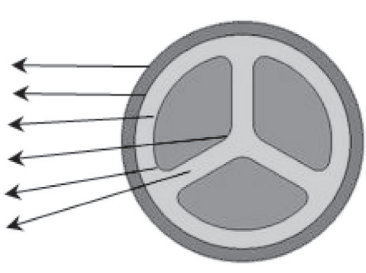


conductor/insulation screen:  $\epsilon_r=1000$ ,  $\sigma=33$  S/m  
 swelling tape:  $\epsilon_r=1000$ ,  $\sigma=100$  S/m  
 conductivities XLPE and filler material are 0 S/m

XLPE, cross-linked polyethylene.

TABLE 2 PILC cable characteristics.

Cable parameters	Value
outer radius earth screen	32.5 mm
inner radius earth screen	29.0 mm
radius conductors	24.0 mm
inner rounding radius conductors outer	5.0 mm
rounding radii conductors	3.0 mm
distance between conductors	5.9 mm
conductivity conductor (Al), $\sigma_{Al}$	$3.69 \cdot 10^7$ S/m
conductivity earth screen (Pb), $\sigma_{Pb}$	$4.70 \cdot 10^6$ S/m
relative permittivity PILC, $\epsilon_{r,pilc}$	3.5-0.1j
conductivity PILC, $\sigma_{PILC}$	0 S/m



PILC, paper-insulated lead-covered.

to the earth screen). The modelled frequency responses are shown in Figure 6 for both the current response and the voltage response. The main content is below 10 MHz and for the PD peak structure the frequency content below 100 kHz is less important. Whether the current or voltage component is measured depends on the type of detector used. In this paper, it is assumed that the signals are detected by means of a high frequency current transformer (HFCT), meaning that it is the PD current that is of interest. The RMU is modelled using the lumped component model shown in Figure 7 and proposed in [15]. Small RMUs are a few metres in size and are modelled as subdivided compartments, each containing a single network component. Usually, they contain one or a few MV cables connected to a busbar and a distribution transformer that feeds a local low-voltage grid. In Figure 7, compartments 1 and 2 contain the cables. Each of them is modelled as a transmission line with its characteristic impedance,  $Z_{c,1}$  and  $Z_{c,2}$  respectively of the XLPE and PILC cables. Inductances  $L_c$  and  $L_{bb}$ , related to loops from the connection to the busbar, are also consid-

ered. Compartment 3 contains the distribution transformer that behaves mainly capacitively at the main frequency components of a PD signal. It is modelled as a capacitance in series with an inductance and a resistance that are, respectively,  $C_{tr}$ ,  $L_{tr}$ ,  $R_{tr}$ . Finally,  $C_{tec}$ ,  $L_{tec}$ ,  $R_{tec}$  represent the cables connecting the transformer to the busbar.

Table 3 shows the parameters of the RMU model obtained averaging the values coming from tests at six RMUs in a frequency range from 200 kHz up to 5 MHz. In Table 3,  $l_{c1}$  and  $l_{c2}$  and  $u_1$  and  $u_2$  are the respective length and propagation speed of the XLPE and PILC cable. The chosen frequency range is the most relevant for the propagation of PD signals in MV cables with a length from hundreds of metres up to several kilometres as shown in [11] and [15]. If the cable to be diagnosed is connected in compartment 1, it is loaded through  $L_c$  and  $L_{bb}$  to the branches representing the cable in compartment 2 and to the parallel branches of the transformer and its connection in compartment 3. Figure 8 shows the impedance of the RMU, seen from the diagnosed cable, with a second connected cable

**TABLE 3** Fitted parameters used for modelling the high-frequency behaviour of an RMU [15].

$Z_{c1}$ ( $\Omega$ ) <sup>1</sup>	$Z_{c2}$ ( $\Omega$ ) <sup>1</sup>	$l_{c1}$ (m)	$l_{c2}$ (m)	$u_1$ (m/s) <sup>1</sup>	$u_2$ (m/s) <sup>1</sup>	$L_c$ ( $\mu$ H)	$L_{bb}$ ( $\mu$ H)	$C_{tr}$ (nF)	$L_{tr}$ ( $\mu$ H)	$R_{tr}$ ( $\Omega$ )	$C_{tcc}$ (nF) <sup>2</sup>	$L_{tcc}$ ( $\mu$ H)	$R_{tcc}$ ( $\Omega$ )
7.9	6.6	425	75	$1.036 \cdot 10^8$	$1.580 \cdot 10^8$	0.34	0.12	2.5	2.6	12	1.9	1.2	8.6

1) Characteristic impedances  $Z_{c1}$  and  $Z_{c2}$  and propagation speeds  $u_1$  and  $u_2$ , obtained from electromagnetic modelling of the cable design for XLPE and PILC respectively (three phases with respect to earth screen).

2) The capacitance  $C_{tr}$  is determined from the cable length (up to 10 m) and its specifications. RMU, ring main unit.

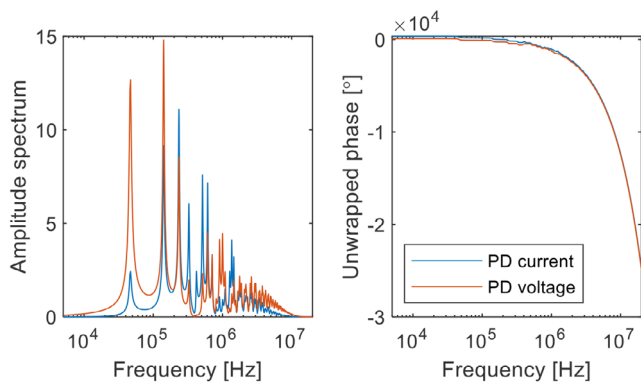


**FIGURE 6** Current (blue) and voltage (red) response upon a delta-function like PD; amplitude spectrum (left) and unwrapped phase angle (right) for a PD at 65 m from the right end of the XLPE cable. XLPE, cross-linked polyethylene.

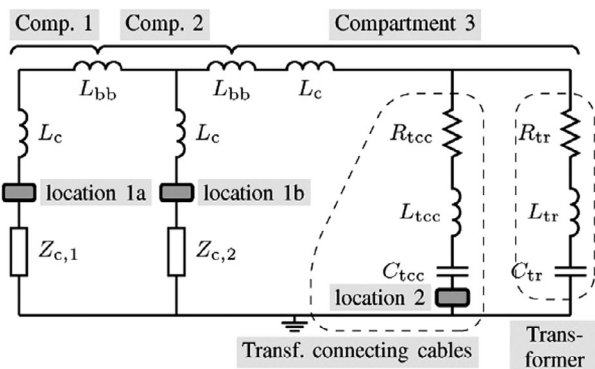


**FIGURE 7** RMU compartment model [15]. RMU, ring main unit.

being either an XLPE or a PILC cable. There are resonances in the low megahertz range caused by the inductances, from the loops formed by the busbar connection, and the capacitances, from the transformer and connecting cables. These resonances, which occur at relevant frequencies for PD signal propagation along the cables, may distort the PD signal waveform. At lower frequencies the impedance of the second connected cable (the PILC cable) dominates the impedance and beyond the resonances, the substation impedance increases due to the inductances.

The adopted RMU model was defined for a frequency range up to about 5 MHz [13]. The modelling of connection details inside RMUs, specific to each RMU, becomes important at frequencies beyond 5 MHz. But these higher frequencies hardly

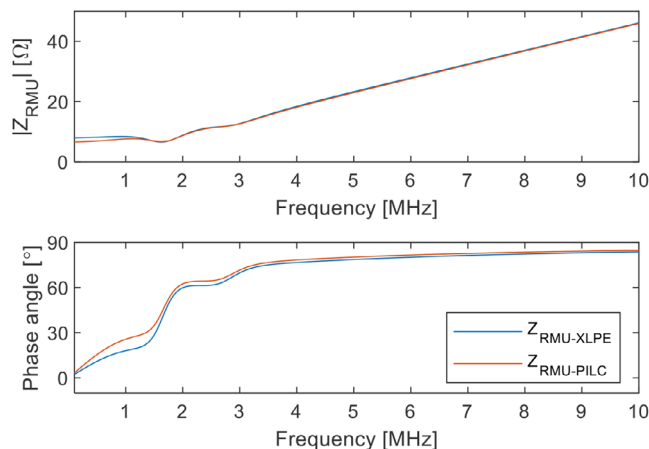


**FIGURE 8** Impedance of an RMU with a distribution transformer and a second connected cable (XLPE or PILC). PILC, paper-insulated lead-covered; RMU, ring main unit; XLPE, cross-linked polyethylene.

contribute due to PD signal attenuation. Therefore, to the aim of power cable diagnostics, the adopted RMU model provides a representative behaviour of the influence of RMUs on PD waveforms.

## 4 | NUMERICAL RESULTS AND ANALYSIS

To test the performance of the EMTR method to localise a PD source in the XLPE cable section of the system under study, a lossless 1D TLM model of the whole system shown in Figure 3 has been developed to perform the time reversal simulations. This distinction is important because it is intended to demonstrate how well a generic model can be used to localise the PD event and show that an exact facsimile of the network under consideration is not necessary.

The DT simulation, during which a PD event is simulated in a point of the system and the PD signals, propagating along the lines, are recorded at the OP, is performed using the lossy model of the system under study (RMU and lines) described in Section 3.

Considering the electromagnetic modelling of the cables reported in Tables 1 and 2 and in Figure 4, in the 1D TLM model the used characteristic impedances of the XLPE and PILC cables and propagation speeds have been evaluated at a frequency of 1 MHz. The characteristic impedances and propagation velocities are close to constant around this

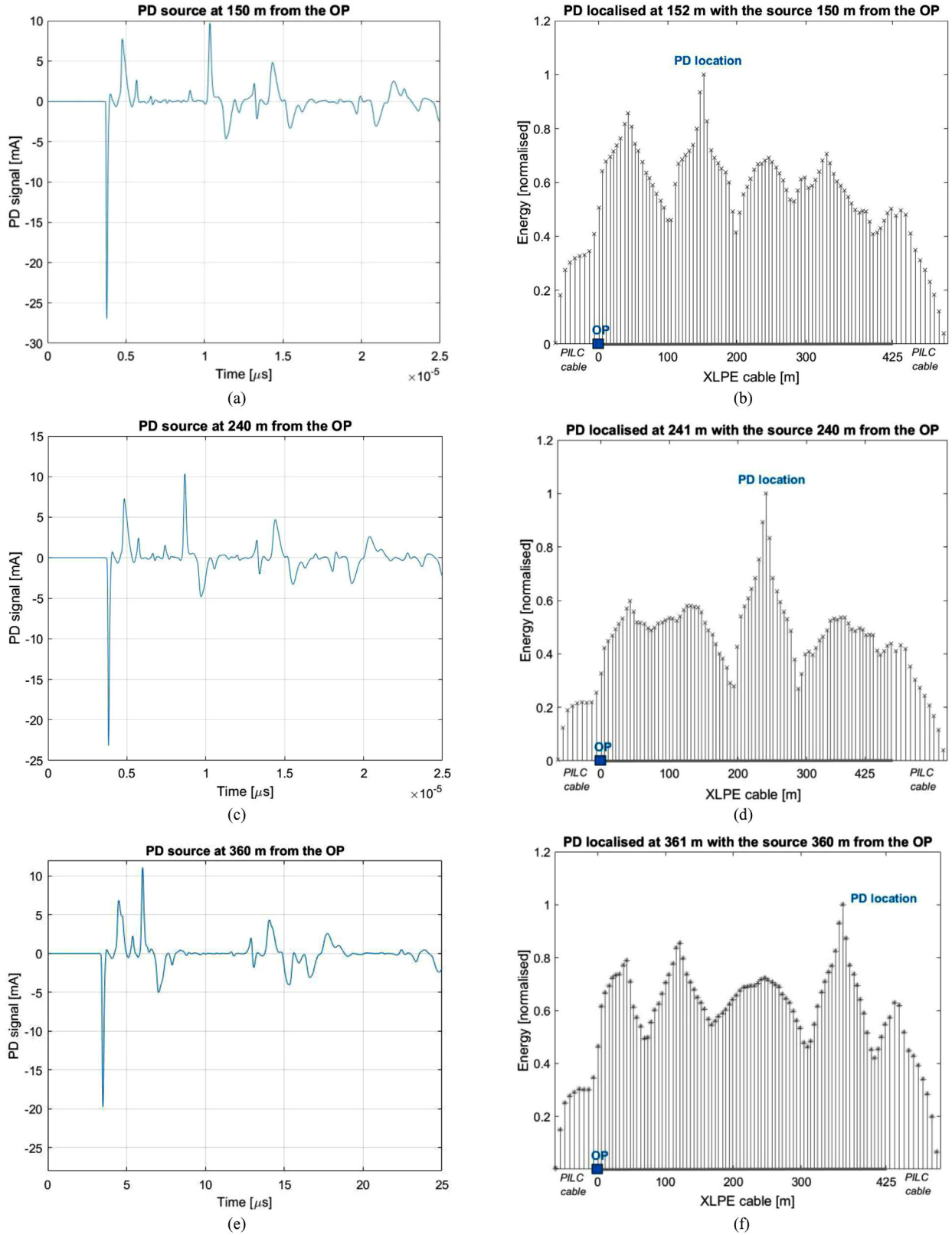


**FIGURE 9** PD signals recorded (simulated) at the OP (on the left) and the EMTR localisation of the PD source in the monitored XLPE cables section (on the right) when the PD source is 150 m, 240 and 360 m away from the OP. EMTR, electromagnetic time reversal; OP, observation point; XLPE, cross-linked polyethylene.

frequency. It is also in the range of relevant signal frequencies for detecting PD signals in power cables [15]. The values are  $Z_{XLPE} = 7.9 \Omega$  and  $v_{XLPE} = 1.036 \cdot 10^8$  m/s,  $Z_{PILC} = 6.6 \Omega$ , and  $v_{PILC} = 1.580 \cdot 10^8$  m/s, respectively, for the XLPE cable and PILC cable, as reported in Table 3.

The RMU was modelled with a 3-m-long TLM model and with a characteristic impedance,  $Z_{RMU}$ , chosen equal to  $Z_{RMU} = 10 \Omega$ , that is, higher than the characteristic impedances of both of the cables connected to it. This is to obtain a relative reflection coefficient  $\Gamma_{RMU} > 0$  because the RMU only causes a distortion mainly for high frequencies and is hardly visible when the wavelengths associated with the remaining frequencies after signal attenuation exceed the RMU size, as explained in [11].

To perform the analysis, the PD signal was collected at the OP, located at the right end of the RMU, in Figure 3, where the XLPE cable under test is connected. Then, the collected PD signal was time reversed and injected into the 1D TLM model and several time reversal simulations were performed. For each PD signal measurement, an initial record length corresponding to a time equal to  $3 \mu\text{s}$  was considered.

In Figure 9 the simulation results of the EMTR-based method are shown when the PD source is located, respectively, at a distance of 150, 240, and 360 m from the OP. In Figure 9, the simulated PD current signals recorded at the OP during the DT simulation in the analysed cases are also reported. Considering the plots (a), (c), and (e) in Figure 9, the interpretation of the individual peaks can become hard since the waveform is affected by several reflections from the relatively short PILC cables. Also, the RMU further disguises individual peak structures. The worst case corresponds to the PD source near the far end of the XLPE cable, that is, 360 m away from the OP and 65 m from the right end of the XLPE cable. In this case, the reflection coming from the PILC cable on its right coincides with the direct PD signal.

For the localisation procedure, a discretisation step of 5 m was chosen between two consecutive positions of the GPDLs moved along the system during the time reversal simulation. This was to provide a trade-off between reasonable resolution and speed of calculation. As Figure 9 shows, the method is able to localise the PD source with a relative error, with respect to the XLPE cable length, of less than 0.1%. Despite the distortion of the PD signal due to the frequency dependence of the system impedances and the reflections coming from the impedance mismatches of the line and the other cable section connected to the RMU, the EMTR-based method is able to localise the source with excellent accuracy. In such configurations the traditional localisation methods based on reflectometry technique are likely to fail.

A total computational time of a few seconds is necessary for localising the PD source, using a 64-bit pc with an Intel® Core™ i7-8700K, CPU at 3.70 GHz, 32 GB RAM and a 1 TB disk. In this case, a time window equal to  $2.5 \mu\text{s}$  was chosen for the PD signal measurement. Such a window is large enough to measure the direct PD signal from the source and the reflections from the other cables considering the propagation speeds for the two cable types. A longer measurement time window

would only increase the computational time of the time reversal simulation without improving the already satisfactory results.

## 5 | CONCLUSION

The question being addressed in this paper was whether EMTR could detect PD events in representative mains configurations, and if so, how well. The performance of the EMTR-based method to localise PDs in the presence of interfering PD reflected signals coming from the impedance discontinuities of the circuit and by the reflections from the cable ends of the PILC cables connected to the RMU was analysed. A description of the EMTR PD localisation method was given and the models used to simulate the grid components, RMU and power cables, useful to reproduce the PD signal distortion were described.

The results show that the EMTR-based method can localise the PD sources in the analysed network configuration where the traditional localisation methods are likely to fail. The numerical results also show that the method is able to localise the PD source in the given configuration with a relative error, with respect to the length of the monitored line section, of less than the 0.1%. The results also showed that the EMTR-based method can localise the PD source using a PD signal measured at a monitoring point located at an RMU somewhere along the line and not necessarily at the line termination. In future works, the presented numerical results will be experimentally verified in a real system.

## AUTHOR CONTRIBUTIONS

Conceptualization (Ideas; formulation or evolution of overarching research goals and aims)—All the authors. Investigation (Conducting a research and investigation process, specifically performing the experiments, or data/evidence collection.)—A. Ragusa and Peter A. A. F. Wouters. Methodology (Development or design of methodology; creation of models.)—All the authors. Validation (Verification, whether as a part of the activity or separate, of the overall replication/reproducibility of results/experiments and other research outputs.)—Visualization (Preparation, creation and/or presentation of the published work, specifically visualization/data presentation)—A. Ragusa and Peter A. A. F. Wouters. Writing—original draft—All the authors. Writing—review & editing—All the authors.

## CONFLICT OF INTEREST STATEMENT

The authors declare no conflict of interest.

## DATA AVAILABILITY STATEMENT

The data that support the findings of this study are openly available in DMU figshare <https://figshare.dmu.ac.uk/> with a DOI: 10.21253/DMU.24624960.

## ORCID

Alistair Duffy  <https://orcid.org/0000-0002-5074-4273>

## REFERENCES

1. Mashikian, M.S., Bansal, R., Northrop, R.B.: Location and characterization of partial discharge sites in shielded power cables. *IEEE Trans. Power Deliv.* 5(2), 833–839 (1990)
2. EN 60270 - High-voltage test techniques—Partial discharge measurements (IEC 60270:2000) – 2001
3. Auzanneau, F.: Wire troubleshooting and diagnosis: Review and perspectives. *Prog. Electromagn. Res. B* 49, 253–279 (2013)
4. Mashikian, M.S., Bansal, R., Northrop, R.B.: Location and characterization of partial discharge sites in shielded power cables. *IEEE Trans. Pow. Del.* 5(2), 833–839 (1990)
5. Robles, G., Shafiq, M., Martínez-Tarifa, J.M.: Multiple Partial discharge source localization in power cables through power spectral separation and time-domain reflectometry. *IEEE Trans. Instrum. Meas.* 68(12), 4703–4711 (2019)
6. Yü, C.C., Rohani, M.N.K.H., Isa, M., Hassan, S.I.S.: Multi-end PD location algorithm using segmented correlation and trimmed mean data filtering techniques for MV underground cable. *IEEE Trans. Dielectr. Electr. Insul.* 24(1), 92–98 (2017)
7. Mohamed, F.P., Siew, W.H., Soraghan, J.J., Strachan, S.M.: Partial discharge location in power cables using a double ended method based on time triggering with GPS. *IEEE Trans. Dielectr. Electr. Insul.* 20(6), 2212–2221 (2013)
8. Wagenaars, P., Wouters, P.A.A.F., van der Wielen, P.C.J.M., Steennis, E.F.: Influence of ring main units and substations on online partial-discharge detection and location in medium-voltage networks. *IEEE Trans. Power Deliv.* 26(2), 1064–1071 (2011)
9. Ragusa, A., Sasse, H., Duffy, A., Rachidi, F., Rubinstein, M.: Electromagnetic time reversal method to locate partial discharges in power networks using 1D TLM modelling. *IEEE L-EMCPA.* 3(1), 24–28 (2021)
10. Ragusa, A., Sasse, H., Duffy, A., Rubinstein, M.: Application to real power networks of a method to locate partial discharges based on electromagnetic time reversal. *IEEE Trans. Power Deliv.* 37(4), 2738–2746 (2022)
11. Ragusa, A., Wouters, P.A.A.F., Sasse, H., Duffy, A.: The effect of the ring mains units for on-line partial discharge location with time reversal in medium voltage networks. *IEEE Access* 10, 33844–33854 (2022)
12. Rachidi, F., Rubinstein, M., Paolone, M.: *Electromagnetic Time Reversal – Application to Electromagnetic Compatibility and Power System.* John Wiley & Sons Ltd, pp. 95–97 (2017)
13. Ragusa, A., Wouters, P.A.A.F., Sasse, H., Duffy, A., Rachidi, F., Rubinstein, M.: Electromagnetic time reversal applied to online partial discharge location in power cables: influence of interfering reflections from the cable circuit. In: 11th International Conference on Computation in Electromagnetics, Cannes, France (2023)
14. Christopoulos, C.: *The Transmission-Line Modeling Method – TLM.* Wiley-IEEE Press (1995)
15. Wagenaars, P., Wouters, P.A.A.F., van der Wielen, P.C.J.M., Steennis, E.F.: Influence of ring main units and substations on online partial-discharge detection and location in medium-voltage networks. *IEEE Trans. Power Deliv.* 26(2), 1064–1071 (2011)

**How to cite this article:** Ragusa, A., Wouters, P.A.A.F., Sasse, H., Duffy, A., Rachidi, F., Rubinstein, M.: Electromagnetic time reversal for online partial discharge location in power cables: Influence of interfering reflections from grid components. *IET Sci. Meas. Technol.* 1–8 (2024).  
<https://doi.org/10.1049/smt2.12197>